

Robert KONOWROCKI
Andrzej CHOJNACKI

ANALYSIS OF RAIL VEHICLES' OPERATIONAL RELIABILITY IN THE ASPECT OF SAFETY AGAINST DERAILMENT BASED ON VARIOUS METHODS OF DETERMINING THE ASSESSMENT CRITERION

ANALIZA NIEZAWODNOŚCI EKSPLOATACYJNEJ POJAZDÓW SZYNOWYCH W ASPEKcie BEZPIECZEŃSTWA PRZED WYKOLEJENIEM W OPARCIU O RÓŻNE METODY WYZNACZANIA KRYTERIUM OCENY*

The article features the results of computer and experimental research on operational issues in the aspect of safety in relation to a freight wagon derailment on a railway track. It presents the knowledge regarding the methods of assessing the operational safety of rail vehicles on railroad tracks for the purpose of comparative analysis. The theoretical analyses were performed based on several methods that assess the safety of their derailments, qualifying for operational reliability, comparing them with the results obtained from experimental research. For the purpose of the research, a computer model of rail vehicle- railway track was created. It took into consideration dynamic parameters of elements used in the real track and rail vehicle. The results obtained from theoretical analyses were validated with experimental tests carried out on real objects (freight vehicle - test track, freight wagon - test rig). As part of the research, new test track geometry for testing rail vehicles was proposed. The results obtained in this way allowed estimating the conditions threatening the operation of a freight vehicle while running on the test rail infrastructure with different assessment criteria and to compare them.

Keywords: *operational safety, rail vehicle dynamics, derailment, experimental tests, numerical investigations.*

W pracy pokazano rezultaty badań komputerowych i eksperymentalnych dotyczących zagadnień eksploatacji w aspekcie bezpieczeństwa w odniesieniu do wykolejenia wagonu towarowego na torze kolejowym. Przybliżono w nim stan wiedzy dotyczącej metod oceny bezpieczeństwa eksploatacji pojazdów szynowych na kolejowych liniach szynowych, w celu ich analizy porównawczej. W pracy wykonano analizy teoretyczne bazując na kilku metodach, które oceniają bezpieczeństwo ich wykolejenia, kwalifikujące się do niezawodność eksploatacyjnej, porównując je z wynikami otrzymanymi z badań eksperymentalnych. Na potrzeby przeprowadzanych badań powstał komputerowy model pojazd szynowy - tor kolejowy. Uwzględniał on parametry dynamiczne elementów zastosowanych w rzeczywistym torze oraz pojeździe szynowym. Otrzymane z teoretycznych analiz wyniki zwalidowano testami eksperymentalnymi wykonanymi na rzeczywistych obiektach (pojazd towarowy - tor testowy, wagon towarowy - stanowisko badawcze). W ramach badań zaproponowano nową geometrię toru testowego do badań pojazdów szynowych. Uzyskane wyniki pozwoliły określić stan zagrożenia eksploatacji wagonu towarowego podczas jazdy po testowej infrastrukturze szynowej przy różnych kryteriach oceny oraz je porównać.

Słowa kluczowe: *bezpieczeństwo eksploatacji, dynamika pojazdów szynowych, wykolejenie, badania numeryczne i eksperymentalne.*

1. Introduction

The problems of safety and reliability of rail vehicles movement is constantly being developed in scientific research [41]. Processes aiming at increasing the level of operational reliability and safety are taken into consideration as early as their design. World trends in this issue require using theories of safety reliability and such vehicles' operational safety [29, 34, 39]. The theory of safety evolved in the 90s so as to counteract risks of failures or accidents which could lead not only to the disruption of a particular technical system functioning but the loss of health, human life or other damage as well [21]. As far as rail vehicles are concerned derailment is the most common kind of accident which causes at the same time the risk of infrastructure degradation, rolling stock or transported cargo damage, disruption of services and environmental damage (the transportation of hazardous

materials) [16, 18]. Therefore the risk determination of such an event occurrence is vital during rail vehicles' tests.

Theoretical analyses and tests are carried out while designing of such vehicles in order to forecast the impact of vehicle parameters on a test track [1, 9, 28] as well as running safety and reliability connected with derailment during movement and monitoring [6, 7]. Then they are continued experimentally in acceptance tests during qualifications to place them in service or after extensive maintenance/modernization of rail vehicles in operation [11, 35]. Safety against derailment is one of primary criteria for assessing the reliability of rail vehicle operation.

Many researchers still deal with the topic of rail vehicle safety [10, 48, 49]. In many cases, the main mechanism causing train derailment is the loss of lateral stability of a railway vehicle [6, 24, 43]. This is caused by a rise in the lateral force value in the wheel-rail contact

(*) Tekst artykułu w polskiej wersji językowej dostępny w elektronicznym wydaniu kwartalnika na stronie www.ein.org.pl

zone. This could be the consequence of various conditions resulting in a loss of lateral guidance provided by the track during normal vehicle operation. The following should be mentioned: climb of the wheel flange, extension of the rail gauge, rail inclination, track condition [49, 50] and reduction of lateral stiffness of the fastening system to sleepers [20].

Apart from theoretical research there are also conducted experimental freight wagons derailment tests [42, 50], where permissible relative wheelset unloading $\lim \Delta q$ was analyzed. The tests showed that unloading may be in the range of $0.62 \leq \lim \Delta q \leq 0.84$. In most cases safety analysis rely on assessment criteria which base on values of Y/Q derailment quotient, wheels unloading and their lift Δz . The review of the literature allows dividing the methodology of safety against railway vehicle derailment at different assessment criteria. The following should be mentioned here:

1. Nadal single-wheel Y/Q limit criterion, – binding for small running speeds on track curves [10].
2. Weinstock axle-sum Y/Q limit criterion, [48].
3. CHXI 50-millisecond time limit- Association of American Railroads (AAR) [12]
4. Y/Q time duration criterion - Japanese National Railways (JNR) [32].
5. Y/Q time duration criterion - Electro-Motive Division (EMD) of General Motors, Inc. [25].
6. Wheel climb distance criterion proposed by Transportation Technology Centre, Inc. (TTCI) [47].

There are several reasons for the risk of rail vehicle derailment to occur. One of the main derailment scenarios takes place when during a vehicle motion a high lateral force acting on the wheelset causes the wheel flange to come into contact with the rail. As a result of this contact, the wheel quickly climbs over the rail and when the maximum value of the flange angle is reached, the wheelset derails. The wheel climb causing derailment is connected with exceeding the limit value of the ratio of lateral force components Y to the vertical force Q at the wheel-rail contact, see Fig. 1. In such a case, the Y/Q force ratio is usually called the derailment quotient.

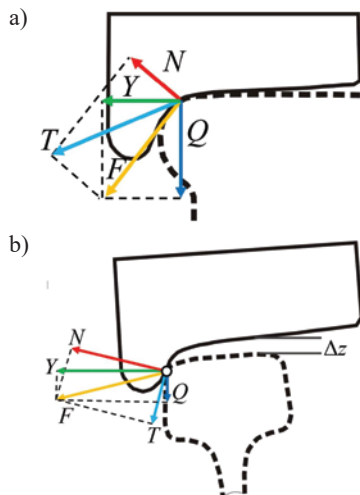


Fig. 1. Force components in the wheel–rail contact on the straight line (a) and on the curve (b): lateral forces (Y), vertical force (Q), normal force (N), lateral rolling friction force (F), flange tilt (γ), wheel lift (Δz)

The values of force components presented in Fig. 1 could be defined as follows:

$$\begin{aligned} Y &= F \cos(\gamma) + N \sin(\gamma) = Y_{\cos} + Y_{\sin} \\ Q &= -F \sin(\gamma) + Q \cos(\gamma) = Q_{\cos} + Q_{\sin} \end{aligned} \quad (1)$$

Nadal criterion [10] defining the derailment quotient is based on the value of friction coefficient μ between wheel and rail as well as flange tilt angle γ . Mathematically, they are determined by (2). This criterion is easy to implement and is therefore widely used to assess safety against derailment.

$$\frac{|Y|}{|Q|} < \frac{\text{tg}\gamma - \mu}{1 + \mu \text{tg}\gamma} \quad (2)$$

In particular, the above criterion is applied to assess the risk of flange climb derailment in UIC 518 Code [46] and European Standard EN14363 [11]. The main modification adopted in these two documents is the requirement that the Y/Q quotient does not exceed the assumed critical value of 1.2 at a distance of 2 m in the vehicle's movement distance interval in the quasi-static tests.

Another standardized [17] index applied to assess rolling stock dynamics related to running safety on 1520 mm gauge tracks is also known. It is called the wheelset stability safety coefficient against derailment in the case of rolling of a wheel flange at/on the rail head and marked with k_z . It is determined from the formula (3). This coefficient is a mathematical modification of the formula (2) and its maximum permissible value for freight wagons is 1.3 [17].

$$k_z < \frac{\text{tg}\beta - f_{FR}\mu}{1 + f_{FR} \cdot \text{tg}\beta} \cdot \frac{P_v}{Y} \geq [k_z], \quad (3)$$

where: β is the tilt angle of the conical part of the rim flange surface to the horizontal reference line, f_{FR} describes the slip friction coefficient in the wheel/ rail contact area, P_v and Y are respectively the vertical and horizontal force components of the wheel interaction on the rail.

The aim of this article is to analyze the safety assessment and thus the operational reliability of rail vehicles against derailment, as well as to propose a new test track geometry that takes into account track twist based on the bogie and vehicle base. Such a track allows determining safety indicators against derailment during one ride of a rail vehicle, without the need for additional tests at stationary stands described in the further section of this paper.

2. Methods of risk assessment and safety against derailment applied during experimental tests

New designs of rail vehicles that will be placed in service in the European Union should meet the essential requirements set out in the Technical Specifications for Interoperability (TSIs). One of the requirements is to check whether the vehicle can be safely operated on the tracks. Both the TSI on freight wagons and the TSI on locomotives and passenger vehicles consider the fulfillment of the requirements given in the EN 14363:2005 standard as proof of safety (the current edition of the standard is EN 14363:2016 [11] – adopted in Poland and marked as PN-EN 14363 + A1:2019-02). Before the adoption of the aforementioned standard, risk and safety tests against goods wagons derailment were carried out based on the requirements provided in the ERRI report (ORE) [40]. No separate requirements were developed to assess the running safety on the twisted track of other rail vehicles. Therefore, the report [40] was also used to determine the safety factor of driving on a twisted track of these vehicles. The standard [11] applies to both quasi-static tests (the speed of the tested rail vehicle does not exceed 10 km/h) and dynamic tests (provided for vehicles with a permissible speed above 60 km/h). This document lists 3 methods for testing operational safety on a twisted track.

Method 1 – vehicle investigations when running on a twisted track. In this case, a track with a constant curve radius $R=150$ m is used as the measuring test rig. Track twist is implemented by chang-

ing the height of the outer rail (positive and negative track cant). The track twist necessary for the test is 3 ‰ over a 30 m section. Moreover, the track construction should reflect the normal conditions of a typical track, taking into account the rail profile, track gauge and maintenance status. During the tests, there must be no lateral forces in the train composition and the vehicle itself must not be braked. The running on the curve is carried out by pushing or pulling the vehicle. The tests are conducted on dry rails so that the wheel/rail coefficient of friction is the highest. The previous document – ORE Report [40] regarding safety tests and dynamics of freight wagons running on a twisted track recommended so that the track be washed with a technical solvent before launching the tests. In the next stage of track preparation, it was required to sprinkle the rail with fine sand and then sweep it off the surface of the rail head. The track prepared in this way ensured a high wheel/rail coefficient of friction.

The European standard [11] lists the mathematical relations from which the twist required on the basis of the bogie and the vehicle base must be determined. If it exceeds 3 ‰, the vehicle must be prepared in a specific way. This can be done, for example, using shims placed under the vehicle suspension. The guidelines for calculating the thickness of the shims and their distribution are given in the annex of EN 14363 standard. Before starting the safety tests, the vertical wheel loads must be determined on the vehicle. Then the test should be planned so that the wheel with the least vertical force is a leading wheel, i.e. a wheel that attacks the outer rail on the measuring curve. If this guideline is not met, this should be done by placing additional shims under the suspension in a different location.

During the investigations, a minimum of 3 tests are required to run the vehicle on the curve at a constant speed not exceeding 10 km/h. The measured parameters include: guiding forces on the inner and outer wheel of a tested vehicle Y_i, Y_a , vertical wheel forces on the inner and outer wheels of the tested vehicle Q_i, Q_a , the angle of attack of the leading wheelset α , leading wheel climb Δz on the entire curve. The abovementioned parameters can be measured by devices placed in the track or on the vehicle. If the measuring devices are placed in the track, their location should be on a twisted track section. Detailed guidelines can be found in the EN 14363:2016 standard [11], and an example of the location of measuring points on the curve of the test track is demonstrated in Figure 6.

The leading wheel lift Δz must be registered in a continuous way. The measurements of forces (Y_i, Q_i) on the inner rail as well as the angle of leading wheelset α serve only to verify the wheel/rail coefficient of friction. On the basis of measured values of vertical Q_a and lateral Y_a forces in selected measuring points on the track curve, running safety quotients $(Y/Q)_a$ were determined. The maximum value of the running safety ratio on a twisted track $(Y/Q)_{a,max}$ was assessed. A vehicle is considered safe if condition (4) is met:

$$\left(\frac{Y}{Q}\right)_{a,lim} \leq \left(\frac{Y}{Q}\right)_{lim} \quad (4)$$

According to Nadal criterion, for the wheel of flank cant of 70° and coefficient of wheel/ rail friction $\mu = 0.36$ this condition is $(Y/Q)_{lim} = 1.2$. If the limit value $(Y/Q)_{lim}$ is exceeded, the wheel climb over the rail head should be checked. If the relation $\Delta z_{max} \leq \Delta z_{lim}$ (where: $\Delta z_{lim} = 0.005$ m) is met, it means that the vehicle has actually not derailed. Therefore this vehicle can be considered safe if it fulfills the following conditions: the flange angle does not exceed 70° in any profile location, then it must be documented that outer rail is dry and it is free of grease or foreign matter, the test has been conducted at least 3 times and in each case the condition $\Delta z_{max} \leq \Delta z_{lim}$ has been met.

Therefore, the final criterion for assessing safety of a vehicle running on the track is the fulfillment of the leading wheel lift criterion $\Delta z_{max} \leq \Delta z_{lim}$.

Method 2 of the rail vehicle derailment risk analysis relates to tests carried out on a test rig simulating the impact of a twisted track on a vehicle and the passage of a test vehicle over a test track without twist. In order to assess the running safety on a twisted track, based on Method 2 - described in the standard [11], two test rigs should be used. The first are special twisting stations, where the minimum wheel force Q_a is determined during running on the twisted track. The second test rig is a track with a radius of $R = 150$ m without cant. At this track, the wheelset maximum guiding force Y_a is determined. In order to determine limit twist, the same relations as described in Method 1 are applied. Due to the fact that the wheel lift up to $\Delta z = 0.005$ m is actually permissible, the dependencies on the limit twists are reduced on the test rig.

The test rig used for measuring wheel force Q_{jk} (j - means wheel set number, k - vehicle side) must be equipped with devices for lifting and lowering them. Independent wheel displacement should be carried out on at least two wheelsets of one bogie. While twisting, Δz_{jk} wheel displacement and the wheel force Q_{jk} of all the wheels are measured continuously. Based on the data processing, taking into account the forces caused by the combined twist of the body and the bogie, the eccentricity of their centers of gravity, including friction and deviations, the minimum vertical wheel force $Q_{jk,min}$ is determined. Figure 2 shows an example of wheel displacement during vehicle twist, performed to determine the value of individual wheel forces on rail tracks. This process carried out on the test rig simulates the change in wheel forces during the vehicle running on a twisted track.



Fig. 2. Positions of suspension beams of measurement modules while conducting tests of freight wagon wheel forces – freight wagon twisting, (a) lifting the wheel over the zero level of the rail head (b) lowering the wheel in relation to the zero level of the rail head

When the maximum guiding force Y_a is determined, the track should consist of a straight section and a curve of a radius $R = 150$ m. The test rig should not have a transition curve, cant or turn. As in Method 1, the track construction should reflect typical track normal conditions taking into account the rail profile, track gauge and maintenance status. Test drives should be planned so as the wheel of minimal vertical force be the leading wheel. In this method, the longitudinal force generated on the train composition must be levelled and the tested vehicle must not be braked. The tests must be carried out at least 3 times at a speed not exceeding 10 km/h. The values measured in this test on a curve include: leading forces on inner and outer wheel of the tested vehicle Y_i , Y_a , the vertical wheel force on the inner wheel of the tested vehicle Q_i and the angle of attack of a leading wheelset α .

The above parameters can be measured by devices placed in the track or on the vehicle. If the measuring devices are placed in the track, their location is in two zones. The first zone is at the beginning of the curve over a distance of more than 3 m up to $2a^*$ ($2a^*$ - bogie centre distance or distance of the axles in non-bogied vehicles). The location of this zone provides the forces measurement during the rotation of the bogie against the body, which is essential for such vehicle constructions. A minimum of 3 measuring points are provided in this zone. The next measuring zone should be located so that the entire vehicle is in the curve. The beginning of the zone should be placed at a distance above $2a^+ + 2a^*$ (with $2a^+$ - as the bogie wheel base) from the beginning of the curve. This zone should also contain a minimum of 3 measurement points.

During the application of this test method, the guiding forces Y_i and Y_a should be recorded for each measurement position. Their assessment should be performed with the use of mean value $Y_{i,med}$ and $Y_{a,med}$ from measurement points separately for each measurement zones. The force direction Y_i in most cases is opposite to force Y_a . Bearing in mind the measured parameters such as (Y_i , Q_i) forces on an inner rail and leading wheelset angle of attack α it is assumed that wheel/rail friction is close to the friction between wheel and rail limit value. Therefore the track should be prepared in a similar way as described in Method 1.

The assessment of meeting the safety requirements and thus minimizing the risk of derailment, while running on a twisted track should be carried out for each wheelset. In this case, in compliance with EN 14363:2016 standard [11], formulas (5) and (6) defining the value of derailment ratio and its limit are applied:

$$\left(\frac{Y}{Q}\right)_{ja} = \frac{Y_{ja,med}}{Q_{jk,min} + \Delta Q_{jH}}, \quad (5)$$

where: $Y_{ja,med}$ is the quasi-static guiding force determined on the basis of the vehicle running on a curve with a radius of $R = 150$ m, $Q_{jk,min}$ denotes the smallest vertical wheel force calculated on the basis of a twist test, ΔQ_{jH} represents the change in the vertical wheel force due to the moment of the guiding forces. The criterion for assessing the derailment risk in this case takes the form of a formula:

$$\left(\frac{Y}{Q}\right)_{ja} \leq \left(\frac{Y}{Q}\right)_{lim}, \quad (6)$$

according to Nadal equation, for a flange angle of 70° and the flange coefficient of friction $\mu = 0.36$. The limit value of derailment quotient is $(Y/Q)_{lim} = 1.2$.

Method 3, covered by standard [11] refers to tests of vehicles on twist test rig and yaw torque test rig. It can be applied for conventional technology vehicles, i.e. those which operate in normal conditions and they or their construction components connected with their running

properties comply with the recognized state of knowledge. Thus they include two-axle bogies, two bogies per vehicle and flange angles of wheels γ between 68° and 70° . Therefore this method cannot be applied for combined-bogie vehicles and rail vehicles fitted with three-axle bogies.

In order to assess the operational safety on a twisted track and the risk of derailment, based on Method 3, two test rigs should be used, i.e. a test rig for measuring wheel force and a test rig for measuring the bogie rotational resistance torque relative to body. The rig used to measure wheel force, as in Method 2, should be equipped with devices for lifting and lowering the wheels. Independent wheel displacement must be carried out on at least two wheelsets of one bogie. The track twist required in the tests is determined from the same formulas as in Method 1. Therefore, the range of wheel displacement during wheel force measurements in Method 3 is greater than the range determined in Method 2. The vehicle wheel force algorithm is the same as in Method 2. During twisting displacement of wheels Δz_{jk} and the wheel force Q_{jk} of all wheels are measured continuously. Based on these data, the vertical wheel force of the tested wheel Q_0 on a levelled track and the wheel force drop ΔQ caused by maximum twist are determined.

The second stage of tests related to measuring the body-to-bogie yaw torque is carried out on a stationary test rig. This position allows the bogie to rotate left and right relative to the body by a given angle. The required rotation speed of the rig is constant and amounts to $1^\circ/s$ within 75% of the bogie rotational angle relative to the body. Due to the load on the wagon during operation, the body-to-bogie yaw torque should be measured for the empty and loaded vehicle. During the test, the bogie should be connected to the vehicle body by all anticipated connections. The essence of this method is to determine the ratio of the leading wheel unloading to the vertical wheel force in the absence of twist and the X factor characterizing the behaviour of the bogie on small radius curves. Permissible values of the above parameters are described by formulas (7) and (8). In compliance with EN 14363:2016 [11], a vehicle is considered safe if it meets two criteria at the same time:

$$\frac{\Delta Q}{Q_0} \leq 0.6, \quad (7)$$

where: ΔQ is the deviation from Q_0 at maximum twist conditions, Q_0 denotes the wheel force for the tested wheelset on levelled track and the bogie rotational resistance factor X for freight wagons depends on axle load. Factor X should be determined depending on:

$$X = \frac{M_{z,Rmin}}{2a^+ 2Q_0}, \quad (8)$$

where: $M_{z,Rmin}$ is the value of the bogie torque relative to the body evaluated at $\psi = a^*/R_{min}$, $2a^+$ denotes distance of wheelsets in a bogie (bogie wheelbase is 1.8 m), $2Q_0$ is wheel force of a tested wheelset. In case of freight wagons, the factor X value is determined from the diagram presenting factor X limit value depending on axle force on a track $2Q_0$ (Fig. 5).

3. Experimental investigation

3.1. Tested object

A typical Eanoss series coal wagon equipped with two standard Y25 bogies was used for experimental research. The tested vehicle is intended for transporting aggregate, coal and bulk materials. It can operate on 1.435 m gauge tracks. The geometrical parameters of the

wagon are: total length with buffers LUP = 14.04 m, maximum width 3.038 m, while the maximum height is 3.43 m. The weight of the tested wagon was 20.3 t. The wagon was designed for a maximum wheelset load of 22.5 t, i.e. up to a gross weight of 90 t. If empty, the wagon can be operated at a maximum speed of 120 km/h, while if loaded - up to 100 km/h.

The parameters necessary to prove that the wagon can be safely operated are: distance between bogie centres $2a^* = 9.0$ m, wheel base distance in a bogie $2a^+ = 1.8$ m.

3.2. Description of the test metod

In order to check if the tested Eanoss series coal wagon can be safely operated, Method 3 specified in EN 14363:2016 standard was used. Two stationary test rigs were used during the experimental tests on the freight wagon. In the first stage of testing it was a test rig for measuring wheel force, while in the second stage for measuring a test rig for measuring the bogie-to- the body yaw torque. Wheel forces measurements were carried out at the TENSAN-PLW test rig, which is capable of independent displacement of individual wheels. At the test rig in question, the Railway Research Institute has its own software, which is used to perform vertical forces of individual wheels during the tests, during which their forces and vertical displacement are recorded. The software used for testing was prepared on the basis of vehicle twist guidelines provided in EN 14363:2016 standard.

The TENSAN-PLW test rig is fitted with specialized measuring modules, which include swingarm pivot mounted in the track axis as seen in Figure 2. Their displacement, relative to the zero track level, is forced by hydraulic cylinders. The location of the measuring modules and their length enables placing each vehicle wheel on them separately, and thus allows individual measurement of their force (Fig. 2). The total length of the test rig is 22.22 m. The range of maximum vertical force on a single swingarm is $Q = 200$ kN and the swingarm displacement is within the range $\Delta h = \pm 0.07$ m. In the case of wheel force measurements of articulated vehicles whose length is greater than the test rig length, the track in front and behind of the test rig is levelled, which allows obtaining a vertical difference in the rails alignment.

3.3. Experimental results

During the tests of the Eanoss series coal wagon, wheel force was measured while lifting and lowering individual wheels from a neutral track level. Two twist tests were carried out, i.e. a test on a fixed wheel set (the tested wheel set which is subject to assessment is not displaced during tests, the wheels in a second bogie are displaced) and a test on a movable wheel set (the tested wheel set is displaced). In the article, in order to limit the number of pages, only the results of the analysis of the wheel forces of the first right front bogie are presented - diagrams in Figure 3. Based on them, the minimum and maximum wheel force ($Q_{0,jkx \min}$ and $Q_{0,jkx \max}$), occurring on a levelled track were determined while twist tests. From the arithmetic mean obtained from these forces, the nominal wheel force was determined without the effect of friction hysteresis, which in the analyzed case was $Q_{0,jkx} = 24.12$ kN. These tests also allowed determining the torsional stiffness of the tested vehicle measured on the base of distance between the spherical pivot $C^*_{tA_{jk}}$ and the axle in the bogie $C^+_{tA_{jk}}$. The above parameters were used to determine the minimum wheel force during the vehicle's ride on the track with a given twist. At a further stage of tests, they were used in theoretical research by implementing them in the numerical model of a freight vehicle presented in Chapter 4 of this article.

The test rig for body-to-bogie yaw torque, belonging to the Railway Institute, was used for testing the aforementioned wagon in the next stage of tests. During tests, the maximum rotation angle of the rig was $\psi = \pm 10^\circ$, whereas the rotation speed was set to three values, i.e. 0.2, 0.6, 1.0 [1°/s]. Finally, in compliance with the standard

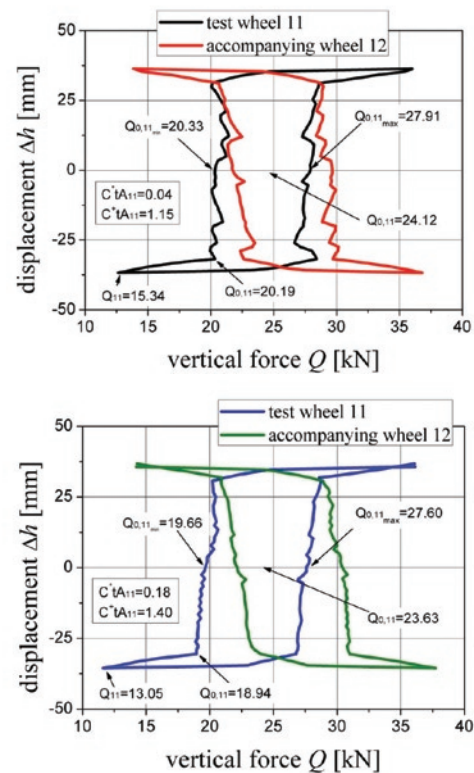


Fig. 3. Measurements of the wheel force on the test rig, measurement on fixed (top) and moving (bottom) wheelset

[11], the results recorded at the rotation speed equal to 1.0 [1°/s] were taken into account for the assessment. Other measurements, which are not subject to assessment, are only used to obtain the appropriate interaction of friction elements to connect the proper measurement of the bogie with the wagon's body. The test was carried out on an empty and loaded wagon, i.e. with a gross load of 89.7 t. At each speed rotation of the bogie relative to the body and for each load of the wagon, one measurement of the body-to-bogie yaw torque was carried out. The results of the resistance torque on the spherical pivot obtained during experimental and simulation tests, with two variants of the wagon load and a rotation speed of 1.0 [1°/s] are shown in the diagrams (Fig. 4).

Measurement of bogie-to-bogie yaw torque relative to freight wagon body, freight wagon empty (left), freight wagon loaded (right) measurement velocity $V_{obr} = 1.0$ [°/s]

The numerical values of the torque at several rotational speeds and different vehicle loads are presented in Table 1. These results were obtained using the assessment criteria according to the limit value of the X factor (Fig. 5). In both load cases, the torque increases as the speed increases during rotation. This indicates a significant impact of degenerative friction between the bogie and the wagon body. The numerical model of the freight wagon used for the simulation tests shown in Figures 4 is described in the further part of the paper.

The aforementioned test rig for dynamic testing of force values in the wheel-rail contact zone was a test track arranged on a radius $R = 150$ m curve over a length of 95 m S-49 rails with a 1:40 inclination, spring-mounted to INBK-7 concrete sleepers with the SB-3 fastening system were used in this track. The spacing of the sleepers is 0.60 m, and the curve uses a nominal track extension of $e = 0.005$ m. Force measurement is performed at the rail level using DC double strain gauges (Fig. 6a) stuck on both rails, located in measuring cross sections 1, 2, 3, 4, 5 and 6 (Fig. 6b). The distance between the measuring cross-sections is determined based on the EN 14363 standard [11]. The value of the wheel force Q is determined from the linear relation

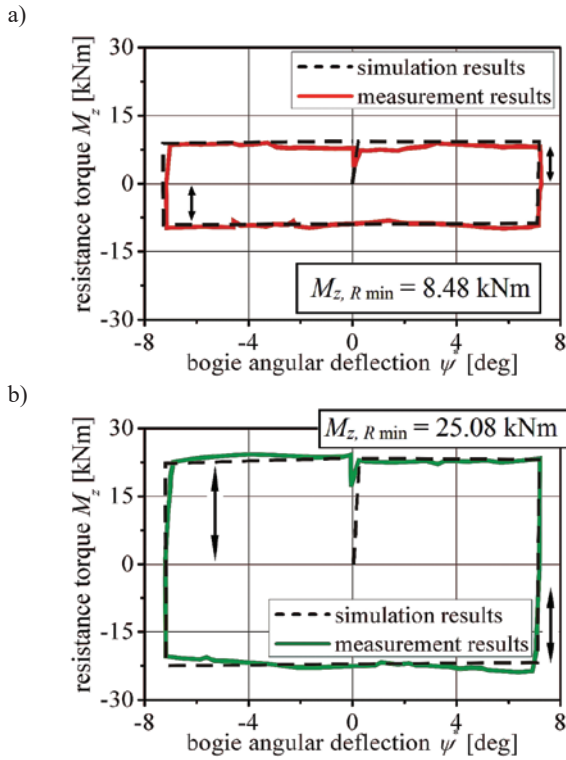


Fig. 4. Limit value of X factor for freight vehicles depending on axle force on the track

Table 1. Measurement results of a freight wagon torque

Bogie type	Wagon loading state	Value of yaw torque $M_{z, R \min}$ [kNm] at different measurement velocities		
		$V_{obr.} = 0.2$ [°/s]	$V_{obr.} = 0.6$ [°/s]	$V_{obr.} = 1.0$ [°/s]
Y25	empty	9.54	8.72	8.48
	loaded	26.07	25.94	25.08

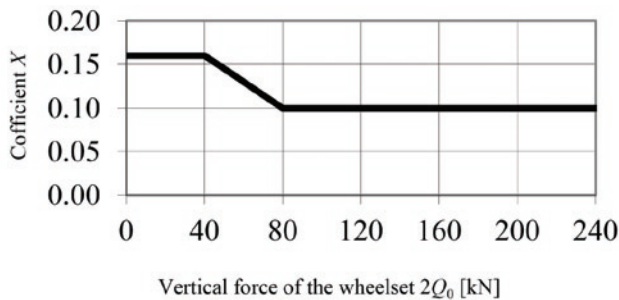


Fig. 5. Location of strain gauges on a rail in a single measuring point (a) and positions of all measurement cross sections 1, 2, 3, 4, 5 and 6 on a tested track curve

of the signals values from the measuring system (strain gauges R_1 and R_2 on the rail neck), which are strengthened by measuring amplifiers dedicated to them.

Linear relation of the measured signal corresponding to the horizontal wheel force Y , correlated with the impact of the vertical wheel force Q impacting the measuring point was determined on a calibration stand and recorded with the formula:

$$\begin{cases} Y_0 = Y - K_0 Q \\ Y_u = Y - K_u Q \end{cases} \quad (9)$$

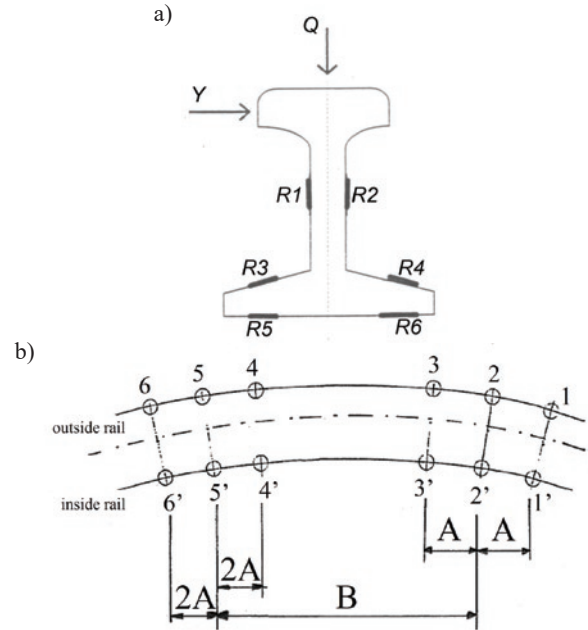


Fig. 6. Lateral forces Y in two measurement cross-sections (2 and 3) when rolling the freight wagon on the test track

where: Y_0 means is the measurement from a double strain gauge stuck to the upper part of the rail foot (strain gauges R_3 and R_4), Y_u denotes the strain gauge from the bottom of the foot (strain gauges R_5 and R_6), Q describes the vertical wheel force interaction on the rail, whereas K_0 and K_u are amplification factors of measuring amplifiers. From the above formulas we obtain (10) determining the value of lateral force Y at the measuring point:

$$Y = \frac{Y_0}{\left(1 - \frac{K_0}{K_u}\right)} - \frac{Y_u}{\left(\frac{K_u}{K_0} - 1\right)} \quad (10)$$

Experimental testing of the Y/Q quotient was carried out when moving a freight wagon along the track at a speed of $v=5$ km/h. Time courses of the Y and Q forces values measured in cross-sections 1, 2, 4, 5 on the outer rail of the track curve and determined from 9 and 10 are presented in diagrams in Figures 7 ÷ 9. Based on the data obtained from each measuring point, the maximum values of derailment quotient for each wheel of a rail vehicle were determined, which are given in Table 2. In this table, the individual wheels of the tested vehicle are marked with the symbol W with indexes i, j . Index i denotes the vehicle axle number, whereas index j the wheelset side ($j=1$ right, $j=2$ left).

Based on the analysis of the results recorded in the given measuring cross-sections during the test runs, the wheelsets of the vehicle bogies were observed to transitionally unload the track laterally. This was caused by different angles of attack between the first and second wheelsets of the given bogie. In the case under analysis, when entering the curve, differences in lateral forces of single bogie sets were noticed at the level of 50% and 36%, respectively in the first and second bogies of the tested wagon (Fig. 7). When exiting the curve, the differences in lateral forces between the sets of a single bogie are much larger and amount to over 60% (Fig. 8). This behaviour of wheel sets also resulted in a reduction in the wheel force of the second wheel sets on the track, which in the analyzed case ranged from 7% to 15% compared to the first set force (Fig. 9).

This behaviour significantly increases the value of the derailment ratio. A similar observation was obtained from the analysis of numeri-

Table 2. Derailment ratio values determined from experimental tests on the track

Wheel W_{ij}	11	12	21	22	31	32	41	42
Y/Q [kN]	0.73	0.72	0.21	0.24	0.59	0.69	0.66	0.62

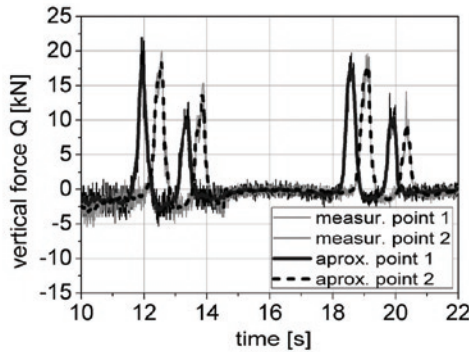


Fig. 7. Lateral forces Y in two measurement cross-sections (4 and 5) when rolling the freight wagon on the test track

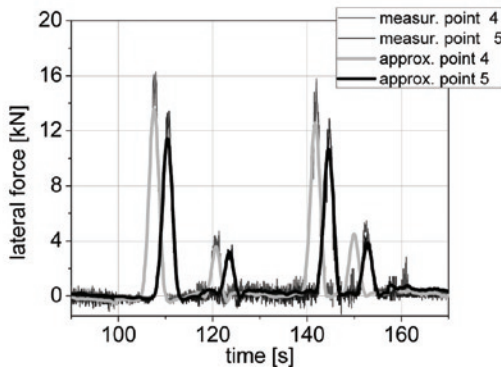


Fig. 8. Vertical forces Q in two measurement cross-sections (4 and 5) when rolling the freight wagon on the test track

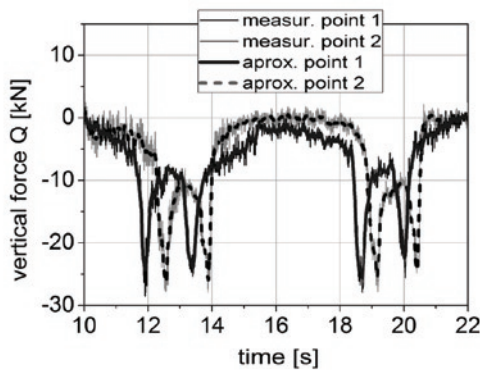


Fig. 9. Vertical forces Q in two measurement cross-sections (4 and 5) when rolling the freight wagon on the test track

cal results performed on the model of the analyzed vehicle described in the next section of the article. The phenomena of the dominant lateral interaction of the attacking wheelset (the first wheelset in the bogie) while negotiating the curve often occurs in rail vehicles [33, 43]. In such conditions, bogies hunting usually occur, and then at the highest lateral instability amplitude the longitudinal symmetry axis of the bogie is deviated from the longitudinal symmetry axis of the track by a certain angle α , called the angle of attack [3, 6, 30]. In this case, the wear of wheelsets and the running surface in the form of polygonization and corrugation also increases [2].

4. Numerical analysis of phenomena accompanying the risk of derailment

4.1. Numerical model of the rail vehicle

In order to determine theoretically the values of forces in the zones of contact between the wheels of the vehicle and the track rails, a model of the wagon mounted on Y25 series bogies was created. The physical model of the vehicle in question was treated as a system of rigid bodies joined together by means of elastic-damping elements (Fig. 10a and 10b). This approach in modeling is called the multi body system method [13,44] and is very often used by researchers in their own codes to analyze rail vehicle dynamics [3,26,45] and in commercial programs, i.e. Vampire, ViGrade/VI-Rail, Autodyn, Simpack, UM Loco. In this method, vehicle structural elements are treated as non-deformable bodies, while suspension elements describe flexible elements [4,8]. Limits of these bodies' motion result from the imposed integrable holonomic constraints [37].

The wagon model considered in the paper was divided into three basic elements, which are wheelsets, bogie frames and a vehicle body. The body was divided into two separate blocks in order to include the experimentally determined body torsional stiffness $K\theta$, in the vehicle model (Fig. 4). The wheelset was described as a block with three degrees of freedom, where lateral displacements were marked with the symbol (y_i) , the angle of attack (ϕ_i) and the galloping (ψ_i) . The index i used in the description of the symbols corresponds to individual wheelsets, assuming the values of $i=1, 2, 3, 4$. The bogie frame is represented by a block with five degrees of freedom, which corresponds to lateral displacement (y_{rj}) , vertical displacement (z_{rj}) , yaw (ϕ_{rj}) , angle of sway (θ_{rj}) and galloping angle (ψ_{rj}) . In this case, the index is $j = 1, 2$, as there are two bogies. In the case of the vehicle body in question, the blocks describing them have five degrees of freedom. These include lateral displacement (y_{nk}) , vertical displacement (z_{nk}) , angle of yaw (ϕ_{nk}) , angle of sway (θ_{nk}) , galloping angle (ψ_{nk}) , at $k=1, 2$ as the body is divided into two blocks. Summing up, the numerical model of the rail vehicle created for research purposes had 64 degrees of freedom.

In the case under consideration, the mathematical model of the freight wagon was described by a system of differential equations, which were derived using Lagrange equations of the second kind. In this approach, generalized coordinates take the form of linear displacements or angles of rotation. The motion of such a vehicle is described by ordinary differential equations of the second order. Assuming that the oscillations of individual blocks of the model relative to the reference system are small, such a system can be written as a linearized system of equations (11) written in the matrix form [14]:

$$[\mathbf{M} d^2/dt^2 + \mathbf{C} d/dt + \mathbf{K}] \cdot \mathbf{q} = \mathbf{F} \quad (11)$$

where: $\mathbf{q} = \{y_v, y_{rj}, y_n, z_{rj}, z_n, \phi_v, \phi_{rj}, \phi_n, \psi_v, \psi_{rj}, \psi_n, \theta_{rj}, \theta_n\}^T$ is vector of generalized coordinates, \mathbf{M} denotes symmetrical inertia matrix, \mathbf{C} is damping matrix, \mathbf{K} is stiffness matrix, \mathbf{F} denotes vector of forces and d/dt is differential operator.

Applying Newton-Raphson methods obtained the system of linear of linear algebraic equations, which is solved in each iteration with a time step $\Delta t = 0.001$ s.

Detailed inertia parameters of the model's elements are presented in Table 3. The wheelbase of the wheelset was 1.5 m, the wheel radius $R = 0.42$ m, the bogies distance of 9 m and the wheelset distance of 1.8 m, the distance of the slide side bearings is equal 1.7 m. The primary suspension stiffness $k_{rx} = k_{ry} = 4000$ kNm and $k_{rz} = 3950$ kNm respectively, the torsion pivot stiffness was assumed at the level $k_x = k_y = k_z = 10$ MNm, the lateral and vertical stiffness of the slide side bearings is $k_{sl_x} = 350$ kNm and $k_{sl_z} = 500$ kNm, respectively. The parameters

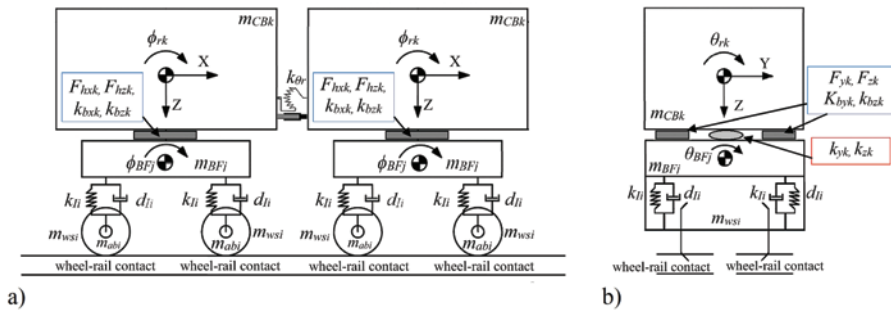


Fig. 10. Physical model of the analyzed vehicle (a) side view, (b) front view of the vehicle

Table 3. Inertia parameters of the freight wagon model

Body	Mass [kg]	I_{xx} [$\text{kg}\times\text{m}^2$]	I_{yy} [$\text{kg}\times\text{m}^2$]	I_{zz} [$\text{kg}\times\text{m}^2$]
body m_{CB}	16000.00	47500.00	51000.00	50050.00
bogie m_{BF}	2000.00	1975.00	2850.00	1560.00
axle box m_{ab}	25.00	10.00	10.00	10.00
wheelset m_{ws}	1300.00	688.00	100.00	688.00

of the bearings were taken from the paper [36]. The bogie pivot is described as a spherical connection with three rotational degrees of freedom, in which the change of friction forces was determined from:

$$F_x = (W_x \cdot \chi) / \sqrt{1 + \left(\frac{Wm_s}{rN_2}\right)^2},$$

$$F_y = (W_y \cdot \chi) / \sqrt{1 + \left(\frac{Wm_s}{rN_2}\right)^2}, \quad (12)$$

$$F_z = (W_z \cdot \chi) / \sqrt{1 + \left(\frac{Wm_s}{rN_2}\right)^2},$$

where: W_x, W_y, W_z denotes torsional speed of the pivot around the axle X, Y, Z; W_m is the absolute speed between the wagon body and the bogie at the central pivot point, χ_s is the tangent at the starting point of the force/speed transfer function of $3.0 \cdot 10^6$ Ns/m, N denotes the normal force directed in the Z, μ_2 is the friction coefficient of 0.19 value, r is the radius of central pivot curvature of 0.19 m [36].

Friction forces F_{bx}, F_{by} in the lateral bearing planes, through which the body was additionally supported on the bogie, was determined from formulas (13) [5]:

$$F_{bx} = (V_x \cdot \chi) / \sqrt{1 + \left(\frac{Wml}{N_1}\right)^2},$$

$$F_{by} = (V_y \cdot \chi) / \sqrt{1 + \left(\frac{Wml}{N_1}\right)^2}, \quad (13)$$

where: V_x, V_y are the relative velocities in the bearing plane in the X, Y directions, Wm denotes the total relative speed on the XY plane, χ describes the tangent at the starting point of the force/speed transfer function of $3.0 \cdot 10^6$ Ns/m, N is the force induced by the weight of the

wagon body operating in the direction normal to the XY plane, μ_1 is the friction coefficient equal to 0.36 [5]. Due to the fact that the paper concerns the analysis of rail vehicle derailment, the structure of the freight wagon model and its mathematical notation are described in the paper generally in the matrix form (11). However, more attention was paid to the description of wheel-rail contact and the methodology for determining forces in the wheel-rail contact zone and derailment ratio resulting from the relations between these forces.

4.2. Wheel-rail contact model

The mathematical model of a freight wagon mounted on Y25 series bogies has been integrated with algorithms and numerical procedures determining the wheel-rail contact. Numerical procedures regarding wheel-rail contact were used to determine the value of forces and areas of their action in contact zones. The contact model was based on Kalker's simplified theory [22] and the FASTSIM algorithm [23]. In order to calculate the tangential contact forces, normal pressure forces were determined, the friction coefficient was adopted at the level of 0.36 [5], the length of the axis a and b of the ellipse of the contact area (Fig. 11a) were calculated using Hertz's theory [19]. Creepage values were considered as relative stiff slip. Relations between these parameters are described by the formula:

$$\begin{matrix} rs_x \\ rs_y \\ rs_z \end{matrix} = \frac{1}{vu_x} \begin{bmatrix} sv_x \\ sv_y \\ sv_y \cdot \sin(|\alpha|) + sv_z \cdot \cos(|\alpha|) \end{bmatrix}, \quad (14)$$

where: rs_x, rs_y are relative stiff slip/creep in longitudinal X and lateral Y directions, rs_z denotes spin, ω describes the contact angle, vu is the speed of the moving reference system, the value of which is equal to the speed of the vehicle, sv denotes the slip speed. Slip speeds sv projected into a given direction were determined from the formula:

$$\begin{matrix} sv_x \\ sv_y \\ sv_z \end{matrix} = \begin{bmatrix} vu_x \\ 0 \\ 0 \end{bmatrix} + \begin{bmatrix} 0 \\ vr_y \\ 0 \end{bmatrix} + \bar{\omega}_w \times \bar{r}, \quad (15)$$

where: $\bar{\omega}_w$ denotes relative \bar{r} angular velocity of the wheel, \bar{r} the coordinate of the contact point in the reference system connected to the centre of wheel mass, vr denotes the relative speed of the centre of wheel mass as defined in the moving reference system.

The next step was to determine tangential contact forces T_x and T_y using the FASTSIM procedure [23]. The algorithm of this procedure divides the elliptical contact zone into smaller areas/cells. In each of these cells, shear stresses and micro-slips are determined in two directions, longitudinal v_x and lateral v_y to the direction of the vehicle ride (Fig. 11b). Then, the contact zones in the contact area at $\gamma = 0$ are determined. The parameters of contact geometry as input quantities for the FASTSIM procedure have been tabulated depending on the lateral displacement of a particular wheel (Fig. 12 and 13), thus the computational time during the simulation of vehicle motion dynamics was reduced.

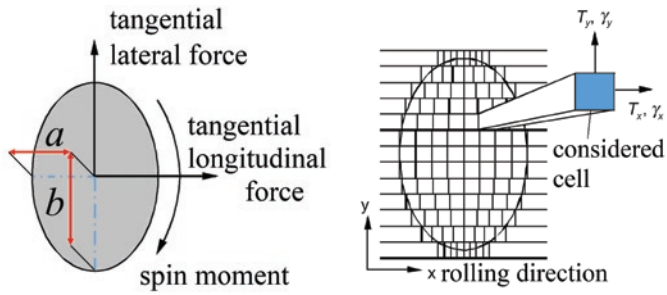
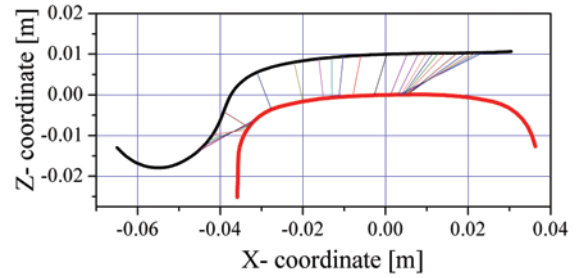


Fig. 11. Tangential forces in the wheel-rail contact zone, half-axes a and b of the contact ellipse and the division of its surface into elements



13. Wheel rail contact position for the wheel profile UIC 60 and rail profile 49E1

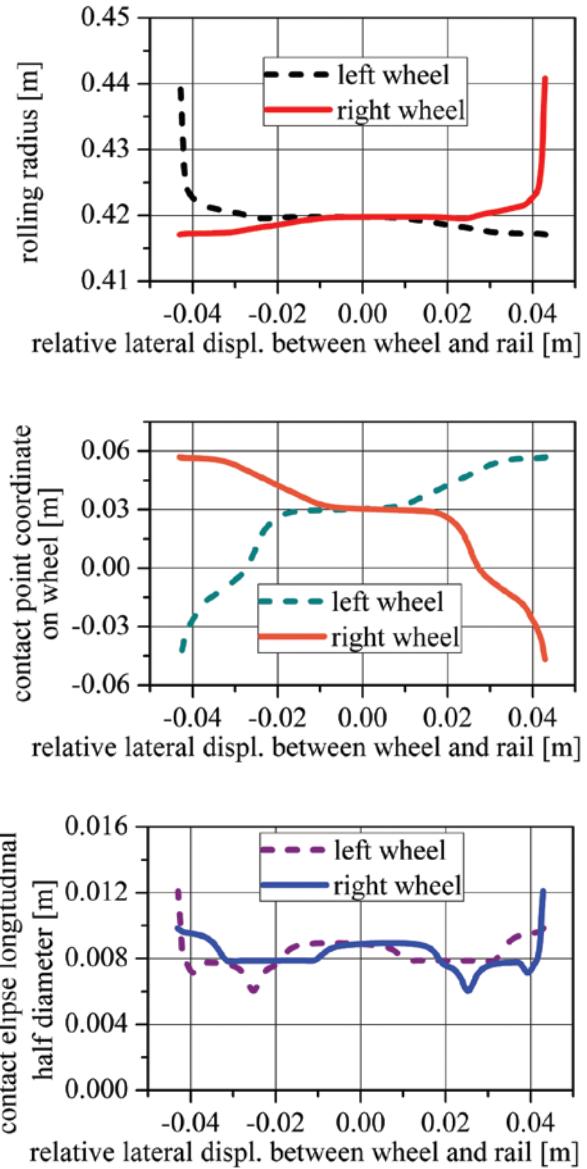
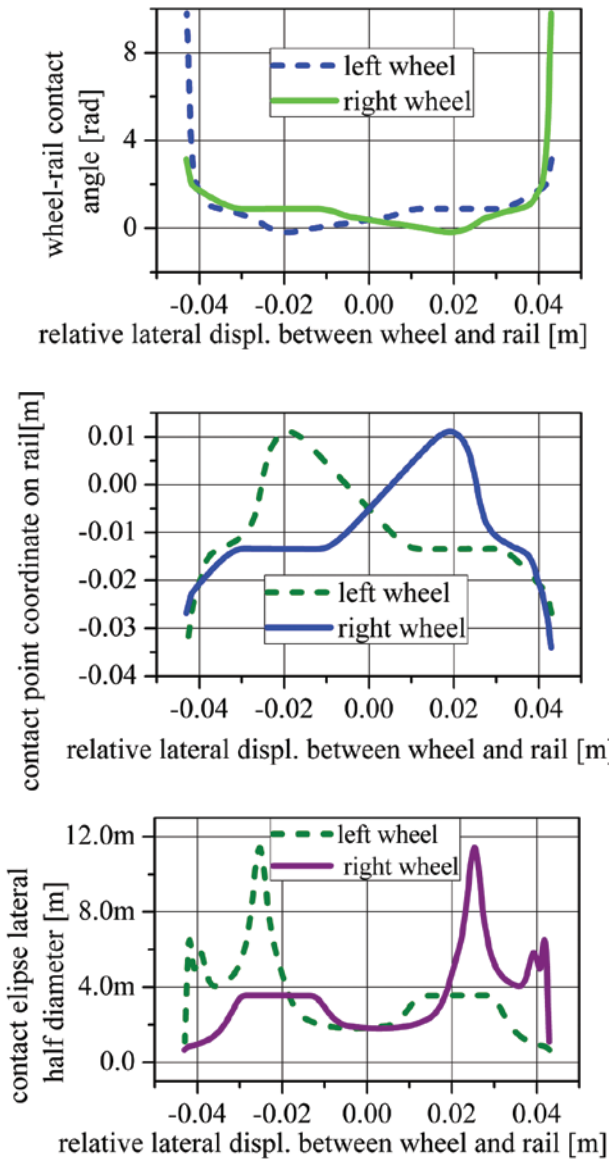


Fig. 12. Parameters of contact geometry of a UIC 60 wheel with a 49E1 rail in the function of lateral displacement y of the wheelset

The further stage of the calculation procedure involves determining and calculating the right sides of the dynamic motion equations (11) for the respective vehicle components and preparing for further solution by numerical integration of these motion equations describing the rail-track system under consideration. The approach described

in this chapter allowed determining the values of forces in the wheel-rail contact zones, which were further used to calculate the value of the Y/Q derailment quotient.

The real nominal profiles of UIC 60 railway wheels and 49E1 rail [38], in the rail inclination configuration in the 1:40 track and shown

in Figure 14 were used in the simulation model for testing the dynamics of the freight wagon.

4.3 Results of numerical investigations

The scope of analyses carried out using the above-mentioned freight wagon-track model relates to the dynamics of the vehicle moving along a curved S-type track with a radius of $R=150$ m and a twist of 3 ‰ (Fig. 12). The track twist enabling tests for the vehicle and the bogie to be determined during a single ride by introducing an additional uplift in the vertical track profile (Fig. 12) was adopted as the original work input for the tests. The most unfavourable variant of the vehicle's operational configuration was adopted during these tests, i.e. the vehicle without a load. During the ride, vertical wheel forces Q and lateral (lateral to the direction of ride) Y in the wheel/rail contact zone are to be recorded. Based on the forces determined in the contact zone, Y/Q derailment quotient is to be determined as the maximum

value of the lateral force to the vertical force. If the value of the Y/Q quotient does not exceed 1.2, the criterion of derailment risk is met. This criterion is based on the balance of forces in the inclined plane of the wheel/rail contact, and its limit value for a given wheel profile and adopted friction coefficient is determined from the formula:

$$\frac{|Y|}{|Q|} < \frac{tg70 - 0.36}{1 + 0.36 \cdot tg70} \quad (15)$$

In the case when the value obtained during dynamic tests is $Y/Q > 1.2$, then the safety against derailment should be additionally checked by the wheel climb. This climb from the zero position should not exceed $\Delta z = 5$ mm. During the numerical simulation, a vehicle travel speed of $v = 5$ km / h was assumed, in accordance with experimental tests (Method 3).

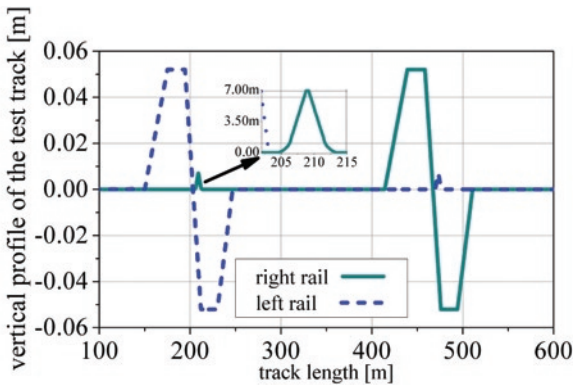


Fig. 14. Geometry of the modified test track with additional twist/lift for a wheelset test

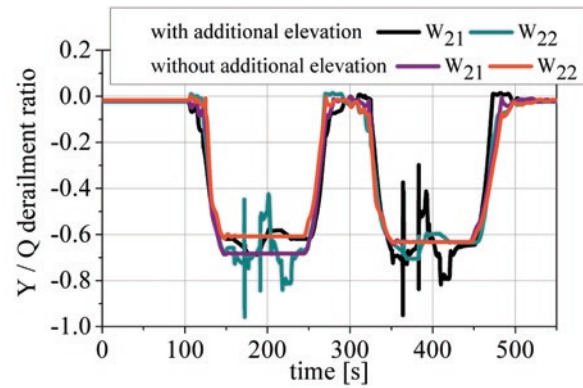
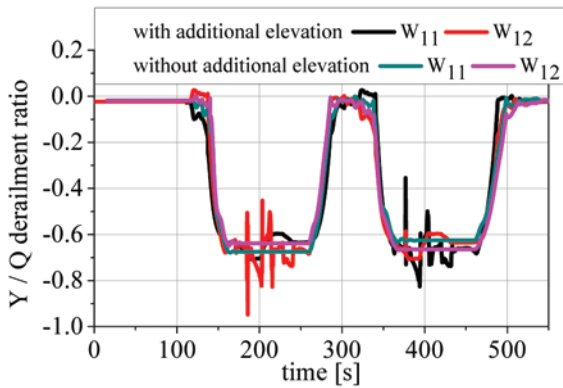
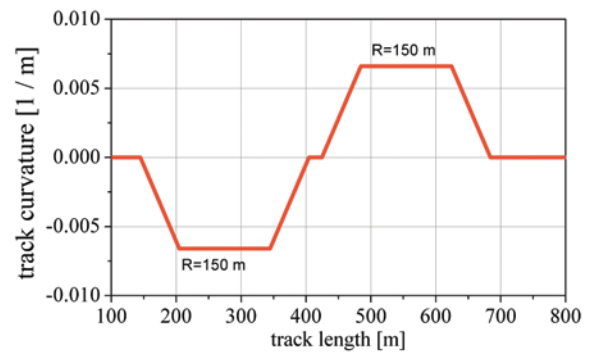


Fig. 15. Derailment quotient obtained from running over a modified test track, guiding wheelset of the first bogie W_{11} and W_{12} and the second wheelset W_{21} and W_{22}

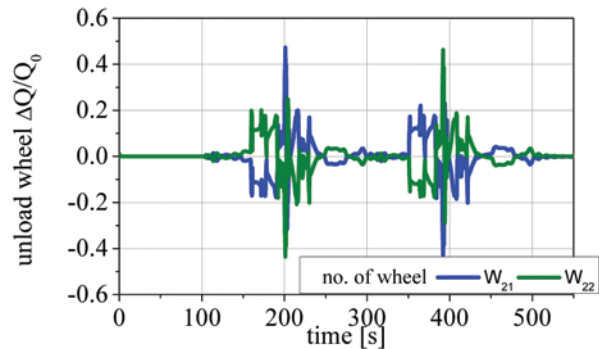
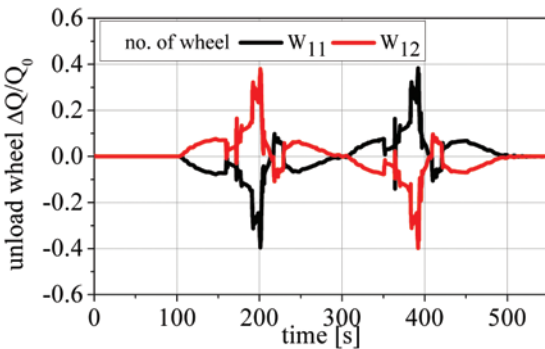


Fig. 16. Unloading the wheels of the wheelset guiding the first W_{11} and W_{12} and the second wheelset W_{21} and W_{22} of the same bogie during the passage along the modified test track

Table 4. Derailment quotient maximum values obtained from numerical investigations and the module of percentage error relative to experimental tests results

Wheel W_{ij}	11	12	21	22	31	32	41	42
Y/Q [kN]	0.67	0.63	0.23	0.27	0.56	0.61	0.68	0.66
Relative error [%]	7.89	12.76	9.52	12.50	5.48	11.46	3.03	6.45

The courses of derailment quotients shown in the graphs (Fig. 15) illustrate the comparison of results of track runs without an additional elevation (dashed curves) and with the elevation corresponding to the track twist based on the wheelbase of a single bogie. It can be observed that the values of the Y/Q quotient for the track without the additional lift have values convergent with the results obtained experimentally (Table 2). In order to verify the correctness of the model operation, the results of the maximum values of the Y/Q derailment quotient obtained during the track run without additional uplift are presented in Table 4. This allowed comparing the experimental tests with the numerical investigations, which results in establishing the module of the relative percentage error between them. The value of this error for individual wheels ranged $3.03 \div 12.76\%$. For wheels on the outer rail track side, the error between results is greater, but does not exceed 13%. The obtained result proves a correctly formulated description of the freight wagon model features and is the basis for establishing correct model validation. A much better quantitative compliance was obtained while determining the resistance yaw torque by comparing the results from numerical investigations and those obtained from the experimental tests described in Chapter 3 (Fig. 4). The created simulation model of the wagon-track system also allows to determine the unloading of the tested vehicle wheels, which is shown in Figures 16, which are also a key indicator of operational safety verification against the derailment.

5. Conclusions and summary

The article features the phenomenon of rail vehicle derailments. Methods of assessing the risk of derailment have been classified basing on a review of literature and standards. The presented description of experimental running safety tests against derailment showed the

methodologies used for their implementation. Obtained and developed results from experimental tests carried out according to the above-described research methods allowed validating the results gained from the numerical investigations of the prepared model. Tests determining the course of derailment quotients' values, wheel unloading and torques were based on a numerical

model describing the experimentally tested freight wagon. The paper also proposes a new, innovative test track geometry for testing safety against derailment. This innovation consisted in the introduction of an additional vertical rise in the rail track acting as twists (Fig. 14), which is based on the vehicle wheel base in a single bogie. The advantage of using in reality such track geometry during real tests, including numerical investigations, may allow reducing the costs of vehicle tests and tests of placing to service by shortening the time of such tests.

This saving results from the fact that three rides were carried out on such a modified real track, without the need for additional tests according to other risk and safety assessment methods against derailment described in Chapter 2 of this paper. The numerical results obtained using a non-linear railway vehicle model demonstrate how operational safety is influenced by various factors related to vehicle and track construction. Based on the conducted research, it has been pointed out that the Y/Q quotient strongly depends on the twist resulting from the bogie base. The analysis of the results obtained from numerical investigations did not indicate a risk of derailment even with a modified track, which was also confirmed by experimental tests carried out according to the described normative methods. An error estimated below 13% between the experimental and theoretical results of the derailment ratio shows high compatibility of the theoretical model with a real rail vehicle. It should also be noted that the difference of the wheelsets angles of attack of a single bogie and the rotation of the bogie relative to the vertical axis has a significant impact on the repeatability of the results achieved.

References

- Bogacz R, Czyczula W, Konowrocki R. Influence of sleepers shape and configuration on track-train dynamics, *Shock and Vibration* 2014; Article ID 393867-1-7: 1-7, <https://doi.org/10.1155/2014/393867>.
- Bogacz R, Frischmuth K. On dynamic effects of wheel-rail interaction in the case of Polygonalisation, *Mechanical Systems and Signal Processing* 2016; 79: 166-173, <https://doi.org/10.1016/j.ymssp.2016.03.001>.
- Bogacz R, Konowrocki R. On new effects of wheel-rail interaction, *Archive of Applied Mechanics* 2012; 82: 1313-1323, <https://doi.org/10.1007/s00419-012-0677-6>.
- Bogdevicius M, Zygiene R. Research of dynamic processes of the system "vehicle - track" using the new method of vehicle wheel with metal scale. *Eksploatacja i niezawodnosc - Maintenance and Reliability* 2018; 20 (4): 638-649, <https://doi.org/10.17531/ein.2018.4.15>.
- Bosso N, Gugliotta A, Somà A. Simulation of a freight bogie with friction damper, *Politecnico di Torino, 5th ADAMS/Rail users conference, Harlem, The Netherlands - May 2000*.
- Chudzikiewicz A, Bogacz R, Kostrzewski M, Konowrocki R. Condition monitoring of railway track systems by using acceleration signals on wheelset axle-boxes, *Transport* 2018; 33; 2: 555-566, <https://doi.org/10.3846/16484142.2017.1342101>.
- Chudzikiewicz A, Opala M. Application of computer simulation methods for running safety assessment of railway vehicles in example of freight cars, *Applied Mechanics and Materials* 2008; 9: 61-69, <https://doi.org/10.4028/www.scientific.net/AMM.9.61>.
- Dailydka S, Lingaitis LP, Myamlin S, Prichodko V. Mathematical model of spatial fluctuations of passenger wagon. *Eksploatacja i Niezawodnosc - Maintenance and Reliability* 2008; 4 (40): 4-8.
- Dyniewicz B, Bajer CI, Matej J. Mass splitting of train wheels in the numerical analysis of high speed train-track interactions, *Vehicle System Dynamics* 2015; 53(1): 51-67, <https://doi.org/10.1080/00423114.2014.982659>.
- Elkins J, Wu H. New criteria for flange climb derailment, *Proceedings of the ASME/IEEE Joint Railroad Conference* 2000; 1-7.
- EN 14363, *Railway applications - Testing for the acceptance of running characteristics of railway vehicles - Testing of running behaviour*

- and stationary tests, European Committee For Standardization, 2016.
12. Federal Railroad Administration. Track Safety Standards, Part 213. Subpart G. September, 1998.
 13. Garcia de Jalon J, Bayo E. Kinematic and Dynamic Simulation of Multibody Systems. Springer-Verlag, 1994, <https://doi.org/10.1007/978-1-4612-2600-0>.
 14. Garg VK, Dukkipati RV. Dynamics of Railway Vehicle Systems. Academic Press 1984, <https://doi.org/10.1016/B978-0-12-275950-5.50014-6>.
 15. Gaspar P, Szabo Z, Bokor J. Observer based estimation of the wheel-rail friction coefficient. IEEE Conference on Computer Aided Control System Design 2006: 1043-1048, <https://doi.org/10.1109/CCA.2006.285990>.
 16. Ge X, Wang K, Guo L, Yang M, Lv K, Zhai W. Investigation on derailment of empty wagons of long freight train during dynamic braking. Shock and Vibration 2018; 18 Article ID 2862143, <https://doi.org/10.1155/2018/2862143>
 17. GosNIIV-VNIIZhT: Norms for analysis and design of railway wagons MPS 1520 mm (not self-propelled). 1996.
 18. He J, Ben-Gera T, Liu X. Risk analysis of freight-train derailment caused by track geometry defect. ASME. ASME/IEEE Joint Rail Conference, 2016 Joint Rail Conference, <https://doi.org/10.1115/JRC2016-5743>.
 19. Hertz H. Über die berührung fester elastischer Körper (On the contact of rigid elastic solids). J. Reine und Angewandte Mathematik 1882; 92: 156-171, <https://doi.org/10.1515/crll.1882.92.156>.
 20. Iwnicki S. (ed.) Handbook of Railway Vehicle Dynamics, CRC Press Inc., 2006, <https://doi.org/10.1201/9781420004892>.
 21. Flammini F. Railway safety, reliability, and security: Technologies and Systems Engineering, IGI Global, 2012, <https://doi.org/10.4018/978-1-4666-1643-1>.
 22. Kalker JJ. Three-dimensional elastic bodies in rolling contact. Springer, 1990, <https://doi.org/10.1007/978-94-015-7889-9>.
 23. Kalker JJ. A fast algorithm for the simplified theory of rolling contact, Vehicle System Dynamics 2007;11 (1): 1-13, <https://doi.org/10.1080/00423118208968684>.
 24. Kardas-Cinal E. Spectral distribution of derailment coefficient in non-linear model of railway vehicle-track system with random track irregularities. ASME. J. Comput. Nonlinear Dynam. 2013;8(3):031014-031014-9, <https://doi.org/10.1115/1.4023352>.
 25. Koci HH, Swenson C A. Locomotive wheel-loading a system approach. General motors electromotive division. LaGrange, IL, February, 1978.
 26. Konowrocki R, Bajer CI. Friction rolling with lateral slip in rail vehicles, Journal of Theoretical And Applied Mechanics 2009; 47(2): 275-293.
 27. Krishna, VV, Berg M, Stiche, S. Tolerable longitudinal forces for freight trains in tight S-curves using three-dimensional multi-body simulations. Proceedings of the Institution of Mechanical Engineers, Part F: Journal of Rail and Rapid Transit 2019, <https://doi.org/10.1177/0954409719841794>.
 28. Krzyżyński T. On continuous subsystem modelling in the dynamic interaction problem of a train-track-system, Vehicle System Dynamics 2007; 24:311-324, <https://doi.org/10.1080/00423119508969633>.
 29. Liu X, Saat MR, Barkan Ch. Freight-train derailment rates for railroad safety and risk analysis. Accident Analysis & Prevention 2017; 98: 1-9, <https://doi.org/10.1016/j.aap.2016.09.012>.
 30. Matej J. Controlled wheel flange climb derailment of the load-measuring wheel set on curved and straight track, Proceedings of the Institute of Vehicles 2015;1(101): 75-90.
 31. Matej J. A new mathematical model of the behaviour of a four-axle freight wagon with UIC single-link suspension. Proceedings of the Institution of Mechanical Engineers Part F-Journal of Rail and Rapid Transit 2011; 225(6): 637-647, <https://doi.org/10.1177/0954409711398173>.
 32. Matsudaira T. Dynamics of high speed rolling stock, Japanese National Railways RTRI Quarterly Reports, Special Issue, 1963.
 33. Matsumoto A, et al. Continuous observation of wheel/rail contact forces in curved track and theoretical considerations, Vehicle System Dynamics 2019; 50(1): 349-364, <https://doi.org/10.1080/00423114.2012.669130>.
 34. Miwa M, Oyama T. Modeling an optimal track maintenance and management strategy in consideration of train derailment accident risk, Journal of Japan Society of Civil Engineers 2019; 75(1): 11-28, <https://doi.org/10.2208/jscejipm.75.11>.
 35. Okamoto I, Uchida M. The coefficient of friction in railway vehicles and tracks. Journal of Japanese Society of Tribologists 2002; 47(4): 249-254.
 36. Opala M. Evaluation of bogie centre bowl friction models in the context of safety against derailment simulation predictions, Archive of Applied Mechanics 2018; 88(6): 943-953, <https://doi.org/10.1007/s00419-018-1351-4>.
 37. Piotrowski J, Październiak P. Influence of dither generated by rolling contact on friction damping in freight wagons, Vehicle System Dynamics 2010; 48: 195-209, <https://doi.org/10.1080/00423111003706722>.
 38. Polish State Railways, Inc.: Instructions Id-1 (D1) - Technical conditions for the maintenance of the surface of the railway lines. Warsaw 2005.
 39. Rausand M. Risk Assessment: Theory, Methods, and Applications, Wiley, 2011, <https://doi.org/10.1002/9781118281116>.
 40. Raport ORE/ERRI B55 Rp.8 - Prevention of derailment of goods wagon on distorted tracks, 1983.
 41. Reliability, Safety, and Security of Railway Systems. Modelling, Analysis, Verification, and Certification, Fantechi A., Lecomte T. Romanovsky A. (Eds.) Second International Conference, RSSRail 2017, Pistoia, Italy, November 14-16, 2017, Proceedings Series Springer Volume 10598, 2017.
 42. Riessbeger K. Zur entgleisungssicherheit der rollenden landstrasse. ZEV Rail Glasers Anna-len. No 2/3 1994.
 43. Sato E, et al., Lateral force during curve negotiation of forced steering bogies, Quarterly Report of RTRI 2003; 44(1): 8-14, <https://doi.org/10.2219/rtriqr.44.8>.
 44. Shabana A. Dynamics of multibody systems. Cambridge University Press, Third Edition, 2005, <https://doi.org/10.1017/CBO9780511610523>.
 45. Szolc, T. Simulation of dynamic interaction between the railway bogie and the track in the medium frequency range. Multibody System Dynamics 2001;6(2): 99-122, <https://doi.org/10.1023/A:1017513021811>.
 46. UIC 518, 2009, Testing and approval of railway vehicles from the point of view of their dynamic behaviour - Safety - Track fatigue - Ride quality.
 47. VII001, AAR Mechanical Division, Manual of Standards and Recommended Practices. Section C- Part II, Volume 1, Chapter XI. Section 11.5.2 Track-Worthiness Criteria, Adopted 1987, Revised 1993.

48. Weinstock H. Wheel climb derailment criteria for evaluation of rail vehicle safety, Paper no. 84-WA/RT-1, 1984 ASME Winter Annual Meeting, New Orleans, LA, November, 1984.
49. Wu H, Wilson, N. Railway vehicle derailment and prevention. In: Iwnicki, S. ed. Handbook of Railway Vehicle Dynamics, Chapter 8, Taylor & Francis, Boca Raton, FL, 2006, <https://doi.org/10.1201/9780849333217.ch8>.
50. Zhou H, Zhang J, Hecht M. Three-dimensional derailment analysis of crashed freight trains. Vehicle System Dynamics 2014; 52(3): 341-361, <https://doi.org/10.1080/00423114.2014.881512>.

Robert KONOWROCKI

Institute of Fundamental Technological Research, Polish Academy of Sciences
ul. Pawińskiego 5B, 02-106 Warsaw, Poland

Railway Institute
ul. Chłopickiego 50, 04-275 Warsaw, Poland

Andrzej CHOJNACKI

Railway Institute
ul. Chłopickiego 50, 04-275 Warsaw, Poland

E-mails: rkonow@ippt.pan.pl, achojnacki@ikolej.pl
